

STUDY OF A NEUTRAL HYDROGEN FEATURE PREVIOUSLY OBSERVED BY CUGNON

I. F. MIRABEL*

*Instituto Argentino de Radioastronomía**, Argentina and
Observatorio Astronómico de la Universidad de La Plata, Argentina*

W. G. L. PÖPPEL*

*Instituto Argentino de Radioastronomía**, Argentina*

and

E. R. VIEIRA

Instituto de Física de la Universidade Federal de Rio Grande do Sul, Brazil

(Received 24 June, 1974)

Abstract. An anomalous velocity cloud near $l=349^\circ$, $b=+3^\circ$, was investigated by Cugnon (1968). The authors made a new set of observations in order to obtain a more complete picture of the feature, including the region originally out of Cugnon's limit of observation. A comparison with optical and radio observations was made and several possibilities of interpretation as to the nature of the object were analyzed.

1. Introduction

Cugnon (1968) studied an extensive neutral-hydrogen feature located outside the galactic plane. He described the object as a cloud having an abnormal radial velocity v of $+50 \text{ km s}^{-1}$ (reduced to the LSR), a velocity dispersion of about 10 km s^{-1} and an H I-mass of $4 \times 10^6 M_\odot$, assuming a distance of 10 kpc. The center of the cloud, as observed by Cugnon, is at $l=349^\circ$, $b=+3^\circ$, not far from the center of the Galaxy. Van der Kruit (1970) made a survey in a region around the galactic center, finding features not associated with the structure in the plane, all at velocities which would be forbidden according to galactic rotation. Following van der Kruit (1971), the observed neutral hydrogen outside the plane – like the cloud studied by Cugnon – can only be explained as being material which has been expelled from the nucleus of our Galaxy, during a more recent active phase. The gas, with a mass of about $10^6 M_\odot$ has not yet reached the plane and has almost no rotation. Its distance from the center is of the order of 2 kpc and the expansion velocities are of the order of 130 km s^{-1} .

Since the object studied by Cugnon could not be observed by him in its whole extension due to Dwingeloo's southern limit of observation, and since it would be interesting to confirm or to reject van der Kruit's hypothesis relating the origin of the cloud, the authors decided to make a new set of observations in order to obtain a more complete picture of the feature.

* Member of the Carrera del Investigador Científico of the Consejo Nacional de Investigaciones Científicas y Técnicas.

** C.C. 5, Villa Elisa, Provincia de Buenos Aires, Argentina.

2. Observations

The observations were carried out with the 30-m telescope at Parque Pereyra Iraola, operated by the Instituto Argentino de Radioastronomía (IAR) and the Carnegie Institution of Washington (CIW). The beamwidth at 21 cm is 0.5° . The instrument is equipped with a 56-channel line receiver, each one 10 kHz wide (velocity resolution $\sim 2 \text{ km s}^{-1}$). The whole system temperature is $\sim 250 \text{ K}$.

The zone of interest lies within $332^\circ \leq l \leq 354^\circ$, $+1^\circ \leq b \leq +7^\circ$. For $b \geq 3^\circ$ we used profiles belonging to a survey made by two of the authors, with a 1° spacing in b and l , not published yet (Pöppel and Vieira, 1971). Complementing this survey, further observations were made by the three authors between November 1972 and July 1973 for $b = +1^\circ$, $+2^\circ$ and some half-degree spaced values of b and l . Also, a few reobservations were necessary in order to extend the original v -ranges of some of the profiles or for improving their noise. In this manner, the profiles of about 170 points in the space were used, each one as the result of at least two measurements, made on different dates, with total integration times not shorter than 12 minutes. Velocities were reduced to the LSR, by using the tables of MacRae and Westerhout (1956). The brightness temperature scale was calibrated by observing the point $l = 356^\circ 00$, $b = -4^\circ 00$, which was assumed to have a peak intensity of 80.0 K (Pöppel and Vieira, 1973).

3. Description of the Results

As an example, an average profile ($l = 349^\circ$, $b = +4^\circ$) is shown in Figure 1. The secondary peak with $T \sim 11 \text{ K}$ at radial velocity $v = +52 \text{ km s}^{-1}$ belongs to the feature studied in this paper. In Figures 2, 3 and 4 some typical contour maps are shown.

From the averaged profiles, the presumed contributions due to Cugnon's cloud were separated by hand. This was straightforward when there was a simple isolated peak at velocities $v \geq +40 \text{ km s}^{-1}$ (as in Figure 1). For the cases where there was superposition of Cugnon's cloud with structures due to the galactic plane, the former was approximated by tracing a Gaussian curve by hand. Observations for $b \leq +1^\circ$ had to be excluded because of the intrinsic complexity of the profiles due to contributions from hydrogen associated with the galactic plane. The same occurred for $b = +2^\circ$, $l = 350^\circ$ to 354° .

Once the presumable contributions due to Cugnon's cloud were separated, their characteristic parameters were obtained: peak velocity v (km s^{-1}), peak temperature T (K), half-width Δv (km s^{-1}) and area under the curve A (K km s^{-1}). The corresponding average uncertainties due to the method employed in the estimation of the feature's contribution, as well as to effects of receiver noise and small errors in the base line determination are estimated to be less than $\pm 1.5 \text{ K}$ for T , $\pm 5 \text{ km s}^{-1}$ for v and $\pm 7 \text{ km s}^{-1}$ for Δv . For A , the mean uncertainty will be of the order of

$$\pm 1.5 \text{ K } \overline{\Delta v} \sim \pm 30 \text{ K km s}^{-1},$$

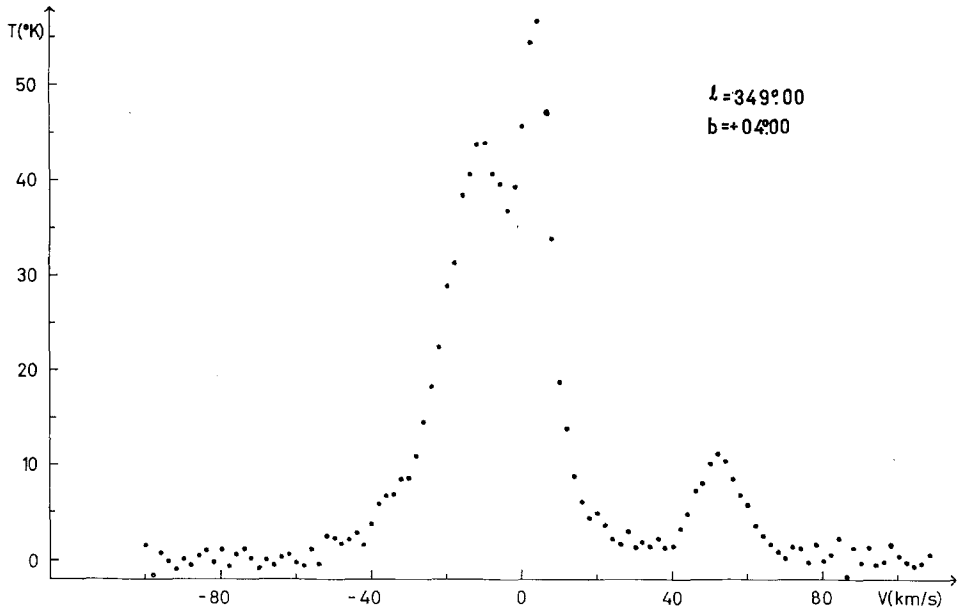


Fig. 1. Hydrogen line profile for $l=349^\circ$, $b=+4^\circ$.

where $\overline{\Delta v} \sim 20 \text{ km s}^{-1}$ is the mean value of Δv over the whole zone where the feature was observed to be present. Clearly, the errors have a stronger relative weight for small values of T and A than for larger ones.

Finally, the number of hydrogen atoms per cm^2 integrated along the line of sight, given by

$$N_{\text{H}} = 1.82 \times 10^{18} A, \quad (1)$$

was computed for each point observed (small optical depths are assumed). As a con-

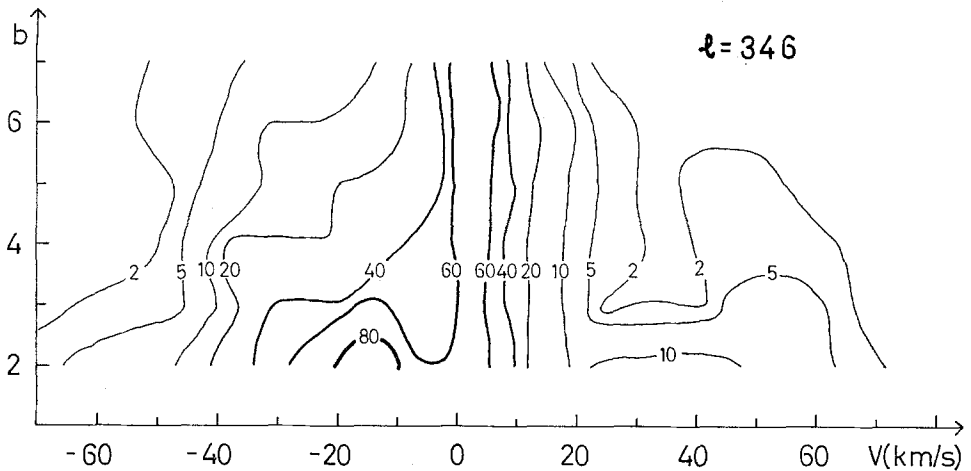


Fig. 2. $b-v$ diagram for $l=346^\circ$. The numbers on the lines are values of brightness temperature in degrees K.

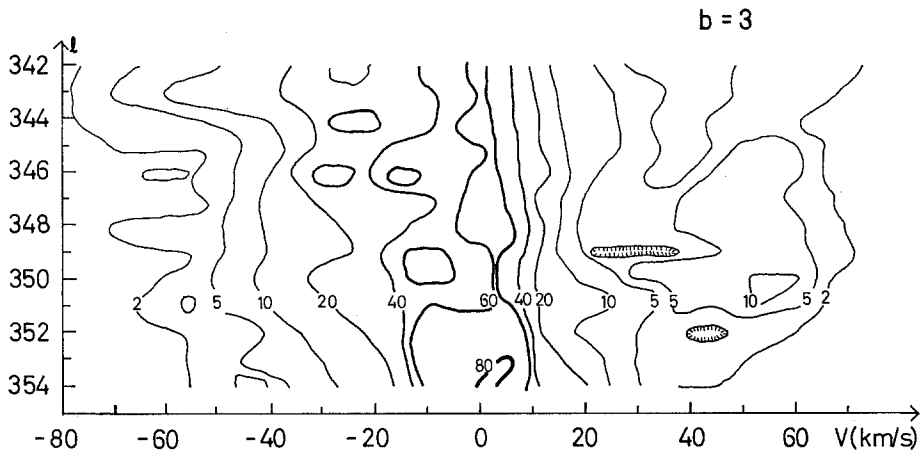


Fig. 3. $l-v$ diagram for $b = +3^\circ$. The numbers on the lines are values of brightness temperature in degrees K.

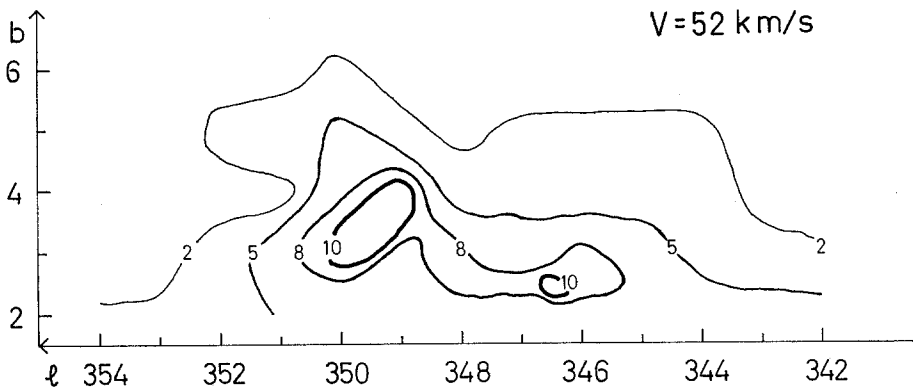


Fig. 4. Lines of equal brightness temperature (in K) for $v = +52 \text{ km s}^{-1}$.

sequence of what was stated above its mean error will be of the order of 0.5×10^{20} atoms cm^{-2} , although this number is somewhat overestimated for small values of N_{H} . Table I gives a summary of the results. In the cases where the peculiar structure of the feature here considered overlapped with that due to plane contributions, Δv was computed by multiplying the semi-half-width, evaluated on the larger velocity side, by 2. Similarly, the areas under the curve were also computed. The distribution of N_{H} as a function of l and b is shown in Figure 5.

The dashed line in Figure 5 is approximately the southern limit of observation in Dwingeloo. As can be seen, the object extends far more to lower longitudes than could originally be observed by Cugnon. The general structure of the isophotes in Figure 5 suggests the separate consideration of two different zones: zone I with $l \geq 342^\circ$ and zone II with $l < 342^\circ$. The isophotes for the former correspond to an elongated object, whose principal axis forms an angle of approximately 26° with the galactic

TABLE I

Summary of the results. Columns 1 and 2 give the galactic coordinates of the observed profiles. Columns 3 to 7 refer to Cugnon's feature. They give the peak velocity v , the peak temperature T , the half-width Δv , the area under the curve A and the corresponding number of hydrogen atoms per cm^2 N_{H} , all computed after the presumable contributions due to Cugnon's feature were separated

l ($^{\circ}$)	b ($^{\circ}$)	v (km s)	T (K)	Δv (km s $^{-1}$)	A (K km s $^{-1}$)	N_{H} (10^{20} at cm^{-2})
354	+3*	52	2.0	15	30	0.6
353	+3*	53	2.0	16	24	0.5
	+4*	46	2.5	16	32	0.6
352	+3*	52	3.8	15	58	1.1
	+4*	47	2.3	26	54	1.1
	+5*	54	1.5	15	30	0.5
351	+3*	53	8.8	18	130	2.4
	+4*	53	3.5	35	104	2.2
	+5*	57	3.0	15	46	0.8
350	+3*	53	9.5	25	160	2.9
	+4*	55	7.0	19	148	2.7
	+5*	53	6.3	21	120	2.2
	+6*	59	3.8	22	52	0.9
349	+2*	58	6.6	14	96	1.8
	+3*	52	7.2	23	176	3.2
	+4*	51	11.3	15	178	3.2
	+5*	54	2.4	21	60	1.1
348.5	+3	56	8.6	21	204	3.7
	+3.5	49	8.2	16	192	3.5
348	+2	56	7.0	24	172	3.1
	+2.5	53	8.6	22	202	3.7
	+3	52	8.2	25	208	3.8
	+4*	48	5.6	30	172	3.1
	+5*	56	1.8	27	48	0.9
	+6*	42	2.4	14	32	0.6
347	+2	49	7.4	29	190	3.5
	+2.5	51	9.7	25	280	5.1
	+3	48	8.2	23	202	3.7
	+4	49	5.6	20	124	2.3
	+5*	50	3.8	21	78	1.4
	+6*	58	2.7	15	50	0.9
346.5	+2	53	6.0	36	336	6.1
	+3	55	7.7	22	192	3.5
346	+2	37	10.0	33	364	6.6
	+2.5	51	8.3	22	236	4.2
	+3	54	8.8	20	166	3.0
	+4	53	4.2	27	110	2.0

Table I (Continued)

l (°)	b (°)	v (km s)	T (K)	Δv (km s ⁻¹)	A (K km s ⁻¹)	N_{H} (10 ²⁰ at cm ⁻²)
	+5	49	4.0	16	72	1.3
	+6*	49	2.3	19	44	0.8
345.5	+2	48	9.2	28	318	5.8
345	+2	40	10.7	25	310	5.6
	+2.5	55	6.4	22	189	3.5
	+3	56	5.2	18	88	1.6
	+4	56	4.0	28	98	1.8
	+5	52	3.8	19	56	1.0
	+6	57	1.7	25	40	0.7
344	+2	46	9.3	22	226	4.1
	+3	52	3.7	22	78	1.4
	+4	54	3.6	16	58	1.1
	+5	48	3.2	24	66	1.2
343	+2	55	7.0	21	170	3.1
	+3	60	3.2	27	90	1.6
	+4	54	2.4	24	48	0.9
342	+2	57	9.6	20	192	3.5
	+3	63	2.9	29	90	1.7
341	+2	63	14.0	16	254	4.6
	+3	62	2.6	20	54	1.0
	+4	63	3.3	16	42	0.8
340	+2	65	7.9	14	150	2.7
	+3	65	1.7	25	42	0.8
	+4	64	3.4	13	50	0.9
339	+2	61	4.3	24	122	2.2
	+3	65	1.1	24	34	0.6
	+4	63	2.3	25	58	1.1
338	+2	64	5.6	17	100	1.8
	+3	62	2.0	22	44	0.8
337	+2	65	5.1	15	72	1.3
	+3	68	2.5	20	44	0.8
336	+2	65	5.0	15	70	1.3
	+3	68	3.1	17	58	1.1
335	+2	65	6.6	15	94	1.7
	+3	62	2.2	16	44	0.8
	+4	64	1.9	12	18	0.3
334	+2	65	4.3	21	78	1.4
	+3	70	1.9	14	28	0.5
333	+2	64	4.1	22	66	1.2
	+3	73	2.7	22	52	0.9
332	+2	61	6.5	22	122	2.2

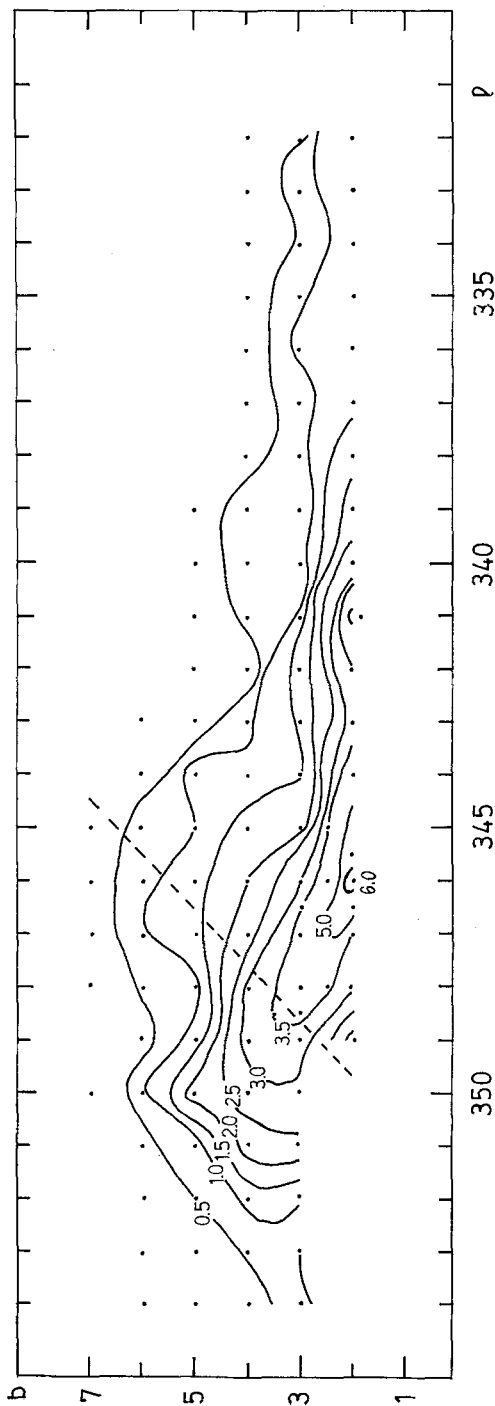


Fig. 5. Lines of equal values of N_H (in units of 10^{20} atoms cm^{-2}).

plane and whose nucleus is located at $l=346^\circ$, $b=+2^\circ$, i.e. below the horizon of Dwingeloo. On the other hand, the isophotes for zone II extend rather parallel to the galactic plane, with a secondary nucleus at $l=341^\circ$, $b=+2^\circ$. These differences in the behaviour of the isophotes show in an indirect way the possibility that region II could eventually not be related to Cugnon's feature, but rather to structures in the galactic plane, with radial velocities similar to that of Cugnon's feature. On the other hand, looking at Table I it can be seen that there are also systematic differences in radial velocities between regions I and II. For $l < 342^\circ$, the values of v in general are higher than for region I. So, we must always have in mind that the isophotes shown in Figure 5 for $l < 342^\circ$ perhaps do not belong to Cugnon's feature. In Section 7c we shall examine this question in more detail.

With the values of N_{H} , the mass M of the object can be computed using the expression

$$M_{(M_\odot)} = 2.44 \times 10^{-18} R^2 \sum \Delta S_i N_{\text{H}_i}, \quad (2)$$

where R (in kpc) is the distance to the Sun, ΔS_i (in square degrees) the area of a surface element on the sky, and N_{H_i} (in atoms cm^{-2}) its corresponding atom density. The summation extends over the whole observed region. The results, computed separately for zones I and II, are, respectively,

$$M_{\text{I}} = 1.9 \times 10^4 R^2, \quad (3)$$

$$M_{\text{II}} = 0.5 \times 10^4 R^2. \quad (4)$$

The first value includes the extrapolated contribution for the region $l=349^\circ$ to 354° between $b=+2^\circ$ and $b=+3^\circ$, left blank in Figure 5. This contribution is less than 8% of the value given in (3).

4. Comparison with Cugnon's Observations

The results given in Table I were compared with those of Cugnon at all points common to both surveys, where the feature is present (23 points marked with * in Table I). For this purpose we averaged the differences between the values of v (radial velocities of the peak), Δv (half-width of the peak) and N_{H} , as given in Table I and the corresponding values obtained by Cugnon, i.e.: \bar{V} (mean radial velocity), σ (velocity dispersion assuming Gaussian shape; we multiplied it by 2.3 in order to make it comparable with Δv) and N'_{H} . The resulting averages for these 23 points in common are the following (standard deviations for the differences are given within parentheses):

$$\begin{aligned} \bar{v} &= 52 \text{ km s}^{-1}, & \overline{v - \bar{V}} &= 2 \text{ km s}^{-1}, & (4 \text{ km s}^{-1}), \\ \overline{\Delta v} &= 20.0 \text{ km s}^{-1}, & \overline{\Delta v - 2.3 \sigma} &= -4.0 \text{ km s}^{-1}, & (6.6 \text{ km s}^{-1}), \\ \overline{N_{\text{H}}} &= 1.5, & \overline{N_{\text{H}} - N'_{\text{H}}} &= -1.1, & (1.8), & (\text{in units of } 10^{20} \text{ cm}^{-2}). \end{aligned} \quad (5)$$

As can be seen, the agreement for the velocities and widths of the peaks is quite

good. For N_{H} the agreement is not so good, Cugnon's values being definitely higher than ours, so that some systematic effect causing the differences in N_{H} might be present. In order to determine this effect, we compared the peak values of the profiles published by Cugnon with those of the survey of Pöppel and Vieira at 48 points in common. The conclusion is that the brightness temperature scale used by Cugnon (bandwidth $B=16$ kHz) renders values $\sim 10\%$ higher than ours ($B=10$ kHz), and $\sim 15\%$ higher than that used in a survey by Braes (1963) (also in Dwingeloo, $B=20$ kHz, 7 common points with Cugnon). The mean difference between Cugnon's values of N_{H} and ours ($\sim 75\%$ of N_{H}) is too high to be due only to scale differences. Perhaps the reason could be related to the fact that Cugnon's observations required a revised zero-correction as a function of altitude, which becomes very important close to the horizon.

5. Comparison with Optical and Radio Observations

The knowledge of its distance is fundamental for the interpretation of the nature and origin of the Cugnon object. Such a knowledge is not directly obtainable from the 21 cm observations, especially since the object has an abnormal radial velocity. Therefore, it is advisable to analyze whatever material in the optical and radio regions is available for the feature.

(a) *Prints of the Whiteoak Zones*

We started first by examining the prints of the Whiteoak Zones in yellow light. No obvious similarity between the optical field and the isolines of Figure 5 could be found. Optically the zone is very complex due to the neighbourhood of the galactic plane.

(b) *Interstellar Absorption Lines*

Optical interstellar lines observed in this region were collected. They are listed in Table II: Columns 1, 2 and 3 give the HD number and the galactic coordinates. Columns 4 and 5 are the optical Ca^+ and, where available, the Na° velocities, both reduced to the LSR. The distance of each star is given in column 6. The corresponding references are given in column 7. The distances were taken from Goniadzki (1972) or, otherwise, they were computed from the corrected distance moduli as given in the references. Results of Table II show that no interstellar absorption lines exist with velocities similar to that of Cugnon's feature.

(c) *H II-Regions*

The atlas of $\text{H}\alpha$ emission by Rodgers *et al.* (1960a) was next investigated. A representation of the $\text{H}\alpha$ emission regions, as taken from this atlas, is given in Figure 6 where we have drawn the isophotes of constant N_{H} from Figure 5 and indicated the stars listed in Table II. Numbers are those assigned in Rodgers's *et al.* (1960b) catalog. As seen from Figure 6, three of their objects fall in our area of observation; their principal characteristics are given in Table III. As can be seen, the radial velocities of the three

TABLE II

Summary of the results referring to the optical interstellar lines observed in the region of interest

HD	l ($^{\circ}$)	b ($^{\circ}$)	Ca^+ (km s^{-1})	Na° (km s^{-1})	r (psc)	Ref.
148 937	336.38	-0.22	-10		1100	BK ^a
149 038	339.4	+2.5	+4	0	1000	BK ^b , G
149 404	340.53	+3.02	-2			BK ^a
149 711	340.38	+2.36	-11		400	BK ^a
151 804	343.6	+1.9	0; 24; -47		1200	BK ^b , G
152 236	343.0	+0.9	-4; -44		1800	BK ^{a,b} , G
154 090	350.8	+4.3	+5.5	+4.5	800	BK ^a , G
154 368	349.95	+3.22	-10		1200	BK ^a
155 450	353.21	+3.92	-2		1000	BK ^a
155 806	352.6	+2.9	+4; -37		1300	BK ^{a,b} , G

BK^a: Buscombe and Kennedy (1962).

BK^b: Buscombe and Kennedy (1968).

G: Goniadzki (1972).

H II-regions are all negative, while the velocity of Cugnon's feature is positive. This fact seems to point out that there is no physical relation of the cloud with these H II-regions.

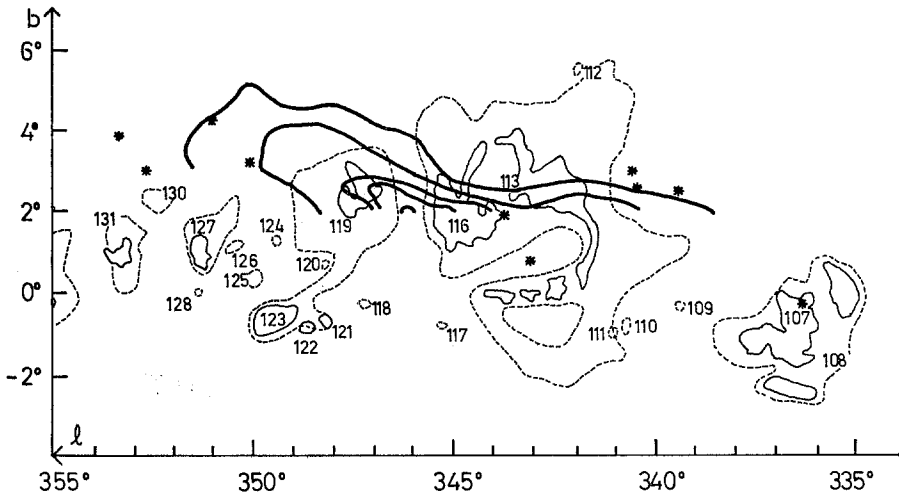


Fig. 6. Superposition of the H α emission regions (Rodgers *et al.*, 1960a) and the isophotes of constant N_{H} from Figure 5 (dark outline). Regions containing H α emission are marked in dashed outline, those of higher intensity in continuous (fine) outline. The * indicate stars from Table II.

TABLE III
Principal characteristics of some H II-regions which are in the zone of interest

1 No.	2 Description	3 Identification	4 Dimensions	5 Center <i>l</i>	6 v_{rad} (km s^{-1})	7 σ (km s^{-1})	8 r_{spectr} (kpc)	9 r_{kin} (kpc)	10 d (pse)	
113	Large loop of ionization in region of fainter emission	NGC 6231 (exciting cluster)	$360' \times 300'$	342.7	+1.8	-19.5	4.0	2.0	2.2	155
116	Concentration inside 113	IC 4628 (exciting cluster)		344.3 (Georgelin and Georgelin, 1970a)	+2.1	-11.3	5.0	1.6	1.7	28
119	Filamentary, with high concentration at $16^{\text{h}}57^{\text{m}}.4$, $-38^{\circ}13'$	Behind cluster NGC 6281; not related to it (Feinstein and Forte, 1975). Exciting star: HD 153 919 (Georgelin and Georgelin, 1970b)	$180' \times 145'$	347.7	+1.9	-8.8	7.0		1.6	24

1 - catalog number; 2 - description of the object; 3 - identification; 4 - angular dimensions; 5 - coordinates of the center. These data were taken from Rodgers's *et al.* (1960b) catalog, unless otherwise indicated; 6 - mean radial velocity corrected to the LSR, as measured on several points on the nebula; 7 - quadratic dispersion; 8 and 9 - the exciting star's spectrophotometric and kinematical distances; 10 - diameter of the H II-region. These data were taken from Georgelin and Georgelin (1970a).

(d) *Radial Velocities of Stars*

For the zone with α_{1900} between $16^{\text{h}}50^{\text{m}}$ and $17^{\text{h}}10^{\text{m}}$ and δ_{1900} between -35° and -40° , the catalog of radial velocities of stars by Abt and Biggs (1972) was investigated. Only two stars appear with radial velocities (reduced to LSR) larger than $+10 \text{ km s}^{-1}$ and no star with $v > 21 \text{ km s}^{-1}$.

(e) *Comparison with the Radio Continuum*

The isolines of Figure 5 were compared with the contour maps of several continuum surveys. At low frequencies, no correlation at all was found by comparison with the following surveys: Hamilton and Haynes (1969a) (10 MHz), Yates *et al.* (1967) (65 MHz), Wielebinsky *et al.* (1969) (85 and 150 MHz), Hamilton and Haynes (1969b) (153 MHz), and the Münster maps at 19.7 and 85 MHz (Altenhoff *et al.*, 1963).

At higher frequencies, the Münster maps at 960 and 1440 MHz show a small nucleus, $1^\circ \times 1^\circ$ wide, centered at $l \sim 345^\circ.5$, $b \sim +1^\circ.5$. The same source can be better distinguished in the following surveys, made with higher resolution: Hill (1969) (1420 MHz, triple source centered at $l = 345^\circ.3$, $b = +1^\circ.5$), Goss and Shaver (1970) (5000 MHz, fourfold source) and Shaver and Goss (1970a) (408 MHz, fifthfold source). The latter authors identify it with the thermal source CTB 35, whose optical identification is the region around IC 4628. As we have seen from Table III it has no relation to

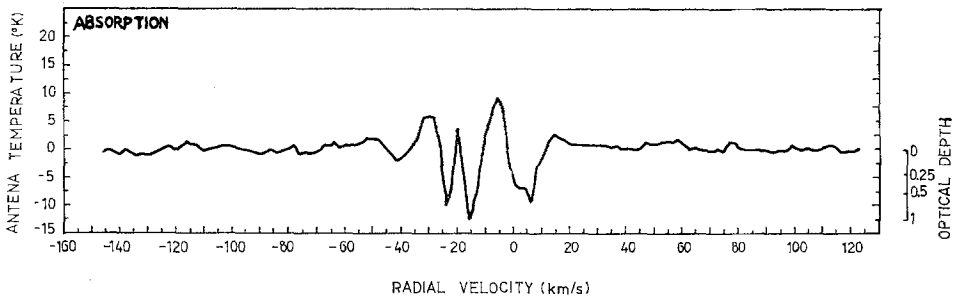


Fig. 7. 21-cm absorption profile for CTB 35 obtained by Radhakrishnan *et al.* (1972).

the object of this paper, since its radial velocity is very different. The same can be concluded from the measurements of the H 109- α line made by Wilson *et al.* (1970).

(f) *21-cm Line in Absorption*

In the direction of CTB 35, 21-cm absorption measurements were made by Radhakrishnan *et al.* (1972) by using filters of 2 km s^{-1} width. The absorption profile obtained by them is reproduced in Figure 7. Radial velocities are relative to the LSR. As can be seen, no absorption is detected in the interval of interest (say from $+30$ to $+60 \text{ km s}^{-1}$).

(g) *Supernovae Remnants*

An examination of the catalog by Ilovaisky and Lequeux (1972) showed that there is only one source which could be related to the cloud because of its position. It is centered at $l=342^\circ.1$, $b=+0^\circ.1$, on the prolongation of the cloud's axis, has a diameter of only $30'$ and a distance to the Sun estimated at 3.1 kpc.

(h) *21-cm Line in Emission*

Inspection of the catalog by Kerr (1969) for the zone $-2^\circ \leq b \leq +2^\circ$ does not show any evident relative absence of hydrogen from the principal structure at lower velocities.

6. Characteristic Parameters for the Object

Before discussing some possible interpretations for the observed object, it will be convenient to define some of its characteristic parameters. These will be given as a function of the principal unknown of the problem: the distance r to the Sun. In order to simplify our analysis we shall consider only region I of the cloud ($l \geq 342^\circ$) and approximate it by a spheroid of radius

$$R = r\sqrt{\varphi_1\varphi_2}, \quad (6)$$

where φ_1 and φ_2 are the apparent semi-axes. From Figure 5 we adopt $\varphi_1=8^\circ$ and $\varphi_2=4^\circ$. In what follows we shall make use of Equation (2) to eliminate the mass M of the cloud from the equations. We define:

(a) a kinetic energy of translation

$$E_{c_{tr}} = \frac{1}{2}MV_t^2 \sim 2 \times 10^{47}r^2 \text{ (kpc)} V_t^2 \text{ (km s}^{-1}\text{) erg}, \quad (7)$$

where V_t is the radial velocity of translation;

(b) an internal kinetic energy

$$E_{c_{int}} = \frac{1}{2}M \frac{(\overline{\Delta v})^2}{2} \sim 2 \times 10^{49}r^2 \text{ (kpc) erg}, \quad (8)$$

where $\frac{1}{2}\overline{\Delta v} = 10 \text{ km s}^{-1}$ is the mean half-width of the profiles;

(c) a transverse radius

$$R = r\sqrt{\varphi_1\varphi_2} \sim 0.1r; \quad (9)$$

(d) an internal gravitational energy (by analogy to sphere-like bodies)

$$E_g \sim -\frac{3}{5}G \frac{M^2}{R} \sim -2.1 \times 10^{47}r^3 \text{ (kpc) erg}; \quad (10)$$

(e) a mean density

$$\bar{\rho} = \frac{M}{4\pi R^3/3} \sim \frac{3 \times 10^{-25}}{r \text{ (kpc)}} \text{ g cm}^{-3}; \quad (11)$$

(f) a characteristic evolution time

$$\tau = \frac{R}{0.5\Delta v} \sim 10^7 r \text{ (kpc) yr.} \quad (12)$$

All these quantities were computed for several values of r (see Table IV). E_c was computed only for distances less than $r=3$ kpc, by adopting for V_r the mean radial velocity of the object, i.e., $\bar{v}=52 \text{ km s}^{-1}$.

TABLE IV

Computed values of some characteristic parameters of the object for several values of its distance r

r (kpc)	M_I (M_\odot)	R (kpc)	$E_{c_{tr}}$ (erg)	$E_{c_{int}}$ (erg)	E_g (erg)	ρ (g cm^{-3})	τ (years)
0.01	1.9	0.001	5.4×10^{46}	2×10^{45}	-2.1×10^{41}	3×10^{-23}	10^5
0.1	1.9×10^2	0.01	5.4×10^{48}	2×10^{47}	-2.1×10^{44}	3×10^{-24}	10^6
1	1.9×10^4	0.10	5.4×10^{50}	2×10^{49}	-2.1×10^{47}	3×10^{-25}	10^7
3	1.8×10^5	0.3		1.8×10^{50}	-5.4×10^{48}	10^{-25}	3×10^7
10	1.9×10^6	1		2×10^{51}	-2.1×10^{50}	3×10^{-26}	10^8
50	4.6×10^7	5		5×10^{52}	-2.5×10^{52}	6×10^{-27}	5×10^8

7. Interpretations

As to the nature of this object, one finds that there are several possibilities: namely,

- (a) an object close to the Sun,
- (b) an object originated in non-local supernovae explosions,
- (c) a distant spiral arm,
- (d) an extragalactic object,
- (e) material falling to the galactic plane,
- (f) material expelled from the galactic center.

Let us investigate now these possible interpretations in detail.

(a) As we have seen in Section 5 the object observed by Cugnon does not seem to be associated either with H II-regions or with associations of stars embedded in ionized gas. If the object were relatively near the Sun, we could consider that the radial translational velocity V_r in (7) is just equal to the observed mean radial velocity, i.e., 52 km s^{-1} . In this manner, the translational kinetic energy would be $\sim 5 \times 10^{50} r^2 \text{ erg}$, with r in kpc. For $r \leq 1.4$ kpc, this energy is comparable with the highest energies involved in explosions of supernovae of type II (Woltjer, 1972). In other words, the maximum distance at which the object could be located if it were the result of a supernova explosion involving an energy equal to or less than 10^{51} erg would be 1.4 kpc. For the

case of a shell, it would be even less, since the total involved H I mass would be larger than the one considered here. On the other hand, the relatively low velocity of the object, for the case of a supernova, would imply a relatively advanced evolutionary phase, like phase III in Woltjer's model. This is in accordance with the values computed for τ in Table IV. Nevertheless, several arguments can be given against an interpretation as a nearby explosion:

(1) No absorption component in the 21-cm line is observed in the velocity interval between +30 and +60 km s⁻¹ in the direction of the thermal radio source CTB 35A ($l=345^{\circ}3$, $b=+1^{\circ}5$) located at a distance of 1.6 kpc (Radhakrishnan *et al.*, 1972), which exceeds the upper boundary given above.

(2) In the catalog by Ilovaisky and Lequeux (1972), the only near positioned supernova remnant is Kes 45 ($l=342^{\circ}1$, $b=+0^{\circ}1$), at a distance of 3.1 kpc. Since this distance is larger than the upper boundary of 1.4 kpc and since its apparent diameter is only 30', it seems improbable that Kes 45 is related to the object under study.

(3) No interstellar lines of positive velocities are seen in early type stars located in the observed region, at distances of the order of 1 kpc (see Table II).

(4) Neither the prints of the Whiteoak Zones nor the H α emission atlas of Rodgers *et al.* (1960a) seem to reveal any evidence about the existence of supernovae remnants in the observed region.

(5) An inspection of the 21-cm line survey by Kerr (1969) does not reveal any notorious absence of low velocity gas in the galactic plane, as would be expected for the case of a big local explosion. Also, no evidence of H I emission at the opposite velocities (~ -50 km s⁻¹) are detected in the region of interest. (See also Figure 1.)

(b) In the preceding subsection, we have considered the case of a supernova explosion involving an energy of 10⁵¹ erg. Let us consider now the case where the object is the whole remnant of a non-local type II supernova explosion (Prata, 1964). Because of the high values of τ in Table IV, we would expect that the shell expansion velocity has fallen down to values comparable to the random motions in the shell, thus giving a single-humped profile. Consequently, for the expansion velocity we adopt now the value

$$\frac{\overline{\Delta v}}{2} = 10 \text{ km s}^{-1},$$

so that, for the same energy, the distance now becomes

$$r \lesssim 7.1 \text{ kpc}.$$

Even for such a distance it would be necessary to explain the positive radial velocity. Another possibility would be to admit that we are dealing with the result of an extraordinarily energetic explosion, such as that of a super-supernova (Shklovskii, 1960), which produces remnants with energies of 10⁵² to 10⁵³ erg.

(c) The fact that the object has an anomalous positive velocity can induce us to inter-

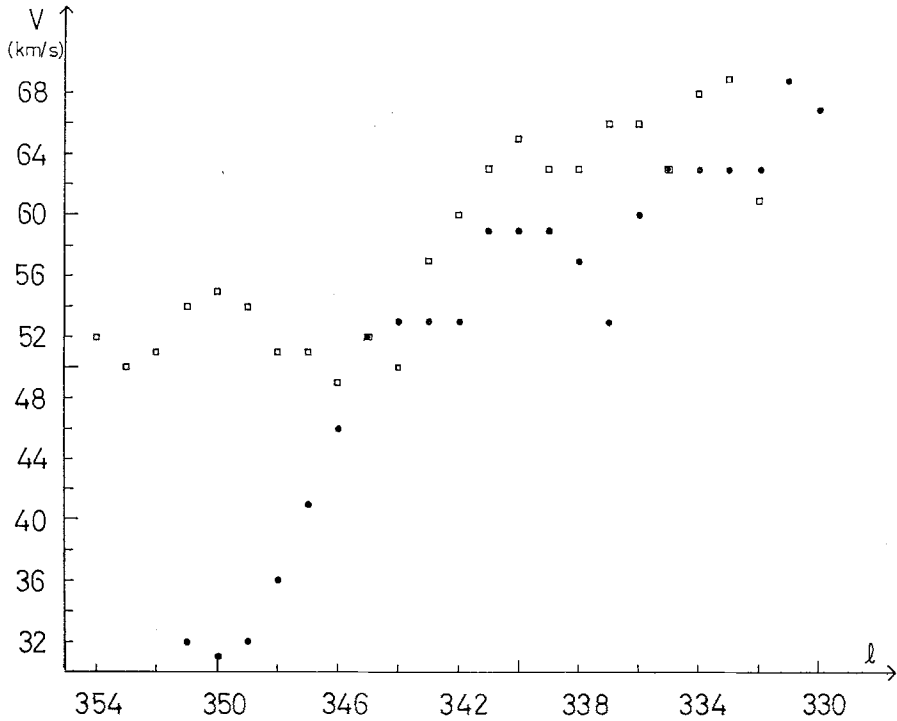


Fig. 8. Comparison of the peak velocities of Cugnon's object, averaged over latitudes between $+2^\circ$ and $+6^\circ$ (squares) with those of a feature of positive velocity (black dots) detected at $b = +1^\circ$ in our profiles.

pret it as a distant spiral arm of our Galaxy. But a short analysis reveals two objections against this hypothesis.

In the first place, the radial velocity variation with longitude does not agree with what would be expected for a distant spiral arm, which rotates regularly in the exterior parts of the Galaxy. In order to show this we compared the velocities of the object with those of a feature of positive velocity which can be detected in our profiles nearest from the galactic plane. In Figure 8 the dots refer to a feature at $b = +1^\circ$, while the squares refer to the peak velocities of Cugnon's object, averaged over latitudes between 2° and 6° . As can be seen, for $l > 342^\circ$ (zone I) the feature's velocity decreases with l , while those of Cugnon's object remain approximately constant. Therefore, it is reasonable to interpret the feature at $b = +1^\circ$ as a galactic spiral arm located at a distance of the order of 20 kpc from the galactic center, according to Schmidt's (1965) model for the mass distribution. The fact that Cugnon's object does not change essentially its velocity with l within zone I would imply an expansion velocity which ought to be very much larger than what could be expected for a far spiral arm. This allows us to reject any relation of Cugnon's object with the feature at $b = +1^\circ$. Moreover, it is interesting to point out that the object with positive velocity

at $b \geq +2^\circ$ in zone II ($l < 342^\circ$) has a different behaviour than at zone I, since in zone II its velocity increases with longitude. This fact makes somewhat doubtful the interpretation for the objects at zones I and II as being parts of one whole system.

The second objection is that the extension of the object in latitude is too large to be a spiral arm, since 5° in latitude at a distance of 20 kpc from the galactic center correspond to an altitude z over the plane of almost 3 kpc.

On the other hand, a strong bending of the galactic plane in the external regions of the Galaxy, as proposed by Verschuur (1973), cannot be excluded. However, the brightness temperatures of the structures considered by Verschuur are very much lower than those observed by us.

(d) A few considerations about the angular size of the object set an upper limit to its distance to the Sun. According to (9), if R would have a value typical for a galaxy of say 20 kpc, r would be equal to 200 kpc, a distance that can be taken as an upper limit. Now, such an object would have to belong to the local group and therefore we would expect some other kind of evidence in the optical or in the radiocontinuum regions. But as we have already seen there is no such evidence. Therefore, this interpretation becomes very doubtful.

(e) A possibility which is worthy of consideration is the case of an object, originating out of the galactic plane, presently moving towards the plane. In particular, because of its coordinates, it could be falling towards the galactic center. If this is the case, it would be located between the Sun and the galactic center and could be an example of material falling from the halo, according to a mechanism proposed by Oort (1966).

If we tentatively apply the virial theorem to this object, by using (8) and (10), it results in a dimension $R \sim 170$ kpc, which clearly suggests that the theorem is certainly not applicable to this case. In other words, the object is not in steady state.

At any rate, no argument can be set either in favour or against the hypothesis of the Cugnon's feature being an object falling to the galactic plane.

(f) If we assume that the object is located near the galactic center, an immediate interpretation could be that it was expelled from there. This idea is founded on the fact that the object could only possess a positive radial velocity and be placed in the region where it is located if it resulted from some explosive event within the galactic nucleus.

That some activity is going on in the galactic nucleus is made probable by two sorts of observations (cf. Oort, 1971). First, there is a non-thermal radio source placed in and around the nucleus. Infrared observations (Becklin and Neugebauer, 1969) have shown that there is a source there, whose spectrum is like that of a Seyfert nucleus, although some 3×10^4 times less intense. The second kind of evidence comes from motions of gas outside the nuclear disk. 21-cm line work made by van Woerden,

Rougoor and Oort (1957) and by Rougoor (1964), has revealed the presence of large expanding motions on the plane in the central part of the Galaxy. Furthermore, van der Kruit (1970) found evidence for possible gas ejection from the galactic nucleus in the form of H I clouds not associated with the plane structure and with velocities which are forbidden for the available galactic rotation models. Cugnon's object is among van der Kruit's evidence. Van der Kruit (1971) made an attempt to explain the gas motion in the central region of the Galaxy through explosive events within the nucleus, by computing the possible orbits. As a particular case, the gas which is observed out of the plane would have been expelled from the nucleus through an angle of 25° to 30° during a recent period of activity ($\sim 6 \times 10^6$ yr ago). The involved kinetic energy is higher than 10^{54} erg.

The projection onto two dimensions of the spatial distribution of the object of our study (Figure 5) and its positive radial velocity allow us to think in terms of an object that was ejected from the galactic center and is now falling towards the galactic plane at the other side of the galactic center, after being ejected from there.

In order to test some other evidence referring to the motion of the cloud, several possible correlations were investigated graphically between N_{H} and Δv , Δv and v and also the spatial distribution of Δv . In no case was there found any positive result.

On the other hand, for the case that the cloud is near to the galactic center, at a distance of, say, 10 kpc from the Sun, its hydrogen mass, dimensions, etc. were computed (Table IV). By taking a translational radial velocity equal to the observed one ($\bar{v} = +52 \text{ km s}^{-1}$), its corresponding kinetic energy amounts to $\sim 5.4 \times 10^{52}$ erg, which fits well in a process like that suggested by van der Kruit.

Summarizing our discussion of the possible interpretations of Cugnon's object we conclude that most probably it was expelled from the galactic center, although the possibility of its being material falling towards that region cannot be excluded. The other possible interpretations which were analyzed turned out to be much more doubtful.

Acknowledgements

We are indebted to Drs H. Marraco and V. Niemelä for helpful comments related to relevant work in the optical region. We thank also Drs J. Sahade and K. C. Turner for reading constructively the manuscript.

References

- Abt, H. A. and Biggs, E. S.: 1972, *Bibliography of Stellar Radial Velocities*, Kitt Peak Natl. Obs.
 Altenhoff, W., Haslam, C. G. T., Large, M. I., Moran, M., and Wendker, H.: 1963, *Mitt. Astron. Instit. Univ. Münster*, No. 9.
 Becklin, E. E. and Neugebauer, G.: 1969, *Astrophys. J.* **157**, L31.
 Braes, L. L. E.: 1963, *Bull. Astron. Inst. Neth.* **17**, 132.
 Buscombe, W. and Kennedy, P. M.: 1962, *Monthly Notices Roy. Astron. Soc.* **124**, 195.
 Buscombe, W. and Kennedy, P. M.: 1968, *Monthly Notices Roy. Astron. Soc.* **139**, 417.
 Cugnon, P.: 1968, *Bull. Astron. Inst. Neth.* **19**, 363.

- Feinstein, A. and Forte, J. C.: 1975, to be published.
- Georgelin, Y. P. and Georgelin, Y. M.: 1970a, *Astron. Astrophys.* **6**, 349.
- Georgelin, Y. P. and Georgelin, Y. M.: 1970b, *Astron. Astrophys. Suppl.* **3**, 1.
- Goniadzki, D.: 1972, *Astron. Astrophys.* **17**, 378.
- Goss, W. M. and Shaver, P. A.: 1970, *Australian J. Phys. Astrophys. Suppl.* **14**, 1.
- Hamilton, P. A. and Haynes, R. F.: 1969a, *Australian J. Phys.* **21**, 895.
- Hamilton, P. A. and Haynes, R. F.: 1969b, *Australian J. Phys.* **22**, 839.
- Hill, E. R.: 1969, *Australian J. Phys.* **21**, 735.
- Ilovaisky, S. A. and Lequeux, J.: 1972, *Astron. Astrophys.* **18**, 169.
- Kerr, F.: 1969, *Australian J. Phys., Astrophys. Suppl.* **9**.
- van der Kruit, P. C.: 1970, *Astron. Astrophys.* **4**, 462.
- van der Kruit, P. C.: 1971, *Astron. Astrophys.* **13**, 405.
- MacRae, D. and Westerhout, G.: 1956, *Table for the Reduction of Velocities to the Local Standard of Rest*, Lund Observatory.
- Oort, J. H.: 1966, *Bull. Astron. Inst. Neth.* **18**, 421.
- Oort, J. H.: 1971, *Nuclei of Galaxies*, North Holl. Publ. Co., Amsterdam, p. 321.
- Pöppel, W. G. L. and Vieira, E. R.: 1971, *Bol. Asoc. Arg. Astron.* **16**, 14.
- Pöppel, W. G. L. and Vieira, E. R.: 1973, *Astron. Astrophys. Suppl.* **9**, 289.
- Prata, S. W.: 1964, *Bull. Astron. Inst. Neth.* **17**, 511.
- Radhakrishnan, V., Goss, W. M., Murray, J. D., and Brooks, J. W.: 1972, *Astrophys. J. Suppl.* **24**, 49.
- Rodgers, A. W., Campbell, C. T., Whiteoak, J. B., Bailey, H. H., and Hunt, V. O.: 1960a, *An Atlas of H- α Emission in the Southern Milky Way*, Mount Stromlo Observatory, Canberra.
- Rodgers, A. W., Campbell, C. T., and Whiteoak, J. B.: 1960b, *Monthly Notices Roy. Astron. Soc.* **121**, 103.
- Rougeor, G. W.: 1964, *Bull. Astron. Inst. Neth.* **17**, 381.
- Rougeor, G. W. and Oort, J. H.: 1960, *Proc. Nat. Ac. Washington, D.C.* **46**, 1.
- Schmidt, M.: 1965, *Stars and Stellar Systems* **5**, 513.
- Shaver, P. A. and Goss, W. M.: 1970a, *Australian J. Phys., Astrophys. Suppl.* **14**, 77.
- Shaver, P. A. and Goss, W. M.: 1970b, *Australian J. Phys., Astrophys. Suppl.* **14**, 133.
- Shklovskii, I. S.: 1960, *Cosmic Radio Waves*, Harvard Univ. Press, Cambridge, Mass.
- Thackeray, A. D.: 1966, *Mem. Roy. Astron. Soc.* **70**, 33.
- Verschuur, G. L.: 1973, *Astron. Astrophys.* **22**, 139.
- Wielebinsky, R., Smith, D. H., and Garzón Cárdenas, X.: 1969, *Australian J. Phys.* **21**, 185.
- Wilson, T. L., Mezger, P. G., Gardner, F. F., and Milne, D. K.: 1970, *Astron. Astrophys.* **6**, 364.
- van Woerden, H., Rougeor, G. W., and Oort, J. H.: 1957, *Compt. Rend. Acad. Sci. Paris* **244**, 1691.
- Woltjer, L.: 1972, *Ann. Rev. Astron. Astrophys.* **10**, 129.
- Yates, K. W., Wielebinski, R., and Landecker, T. L.: 1967, *Australian J. Phys.* **20**, 595.